Interferometric method for phase calibration in liquid crystal spatial light modulators using a self-generated diffraction-grating

José Luis Martínez Fuentes,[1,2,3] Enrique J. Fernández,[2] Pedro M. Prieto,[2] and Pablo Artal[2]

[1]*Instituto de Investigación en Óptica y Nanofísica, Laboratorio de Óptica, Universidad de Murcia, Edificio 34, Campus de Espinardo, 30100 Murcia, Spain*
[2]*Departamento de Ciencia de Materiales, Óptica y Tecnología Electrónica, Universidad Miguel Hernández de Elche, 03202 Elche, Spain*
[3]*jose.martinez@umh.es*
[4]*enriquej@um.es*

Abstract: An auto-referenced interferometric method for calibrating phase modulation of parallel-aligned liquid crystal (PAL) spatial light modulators (SLM) is described. The method is experimentally straightforward, robust, and requires solely of a collimated beam, with no need of additional optics. This method uses the SLM itself to create a tilted plane wave and a reference wave which mutually interfere. These waves are codified by means of a binary diffraction grating and a uniformly distributed gray level area (piston) into the SLM surface. Phase shift for each gray level addressed to the piston section can then be evaluated. Phase modulation on the SLM can also be retrieved with the proposed method over spatially resolved portions of the surface. Phase information obtained with this novel method is compared to other well established calibration procedures, requiring extra elements and more elaborated optical set-ups. The results show a good agreement with previous methods. The advantages of the new method include high mechanical stability, faster performance, and a significantly easier practical implementation.

OCIS codes: (230.6120) Spatial light modulators; (120.2040) Displays; (060.5060) Phase modulation; (110.1080) Active or adaptive optics; (160.3710) Liquid crystals; (120.3180) Interferometry.

References and links

1. G. Lazarev, A. Hermerschmidt, S. Krüger, and S. Osten, "LCOS spatial light modulators: Trends and applications," in W. Osten, ed., *Optical Imaging and Metrology* (Wiley-VCH, 2012), Chap. 1.
2. M. Kujawinska, R. Porras-Aguilar, and W. Zaperty, "LCOS spatial light modulators as active phase elements of full-field measurement systems and sensors," Metrol. Meas. Syst. **19**, 445–458 (2012).
3. P. Prieto, E. Fernández, S. Manzanera, and P. Artal, "Adaptive optics with a programmable phase modulator: applications in the human eye," Opt. Express **12**(17), 4059–4071 (2004).
4. E. J. Fernández, P. M. Prieto, and P. Artal, "Wave-aberration control with a liquid crystal on silicon (LCOS) spatial phase modulator," Opt. Express **17**(13), 11013–11025 (2009).
5. E. J. Fernández, P. M. Prieto, and P. Artal, "Binocular adaptive optics visual simulator," Opt. Lett. **34**(17), 2628–2630 (2009).
6. E. J. Fernández, P. M. Prieto, and P. Artal, "Adaptive optics binocular visual simulator to study stereopsis in the presence of aberrations," J. Opt. Soc. Am. A **27**(11), A48–A55 (2010).
7. C. Cánovas, P. M. Prieto, S. Manzanera, A. Mira, P. Artal, and P. Artal, "Hybrid adaptive-optics visual simulator," Opt. Lett. **35**(2), 196–198 (2010).
8. A. M. Weiner, D. E. Leaird, J. S. Patel, and J. R. Wullert, "Programmable femtosecond pulse shaping by use of a multielement liquid-crystal phase modulator," Opt. Lett. **15**(6), 326–328 (1990).
9. T. J. McIntyre, C. Maurer, S. Bernet, and M. Ritsch-Marte, "Differential interference contrast imaging using a spatial light modulator," Opt. Lett. **34**(19), 2988–2990 (2009).
10. A. Hermeschmidt, S. Krüger, T. Haist, S. Zwick, M. Warber, and W. Osten, "Holographic optical tweezers with real-time hologram calculation using a phase-only modulating LCOS-based SLM at 1064 nm," Proc. SPIE **6905**, 690508 (2008).

#265379 Received 18 May 2016; revised 10 Jun 2016; accepted 10 Jun 2016; published 15 Jun 2016

11. L. Lobato, A. Márquez, A. Lizana, I. Moreno, C. Iemmi, and J. Campos, "Characterization of a parallel aligned liquid cristal on silicon and its application on a Shack-Hartmann sensor," Proc. SPIE **7797**, 77970Q (2010).
12. J. L. Martínez, I. Moreno, M. del Mar Sánchez-López, A. Vargas, and P. García-Martínez, "Analysis of multiple internal reflections in a parallel aligned liquid crystal on silicon SLM," Opt. Express **22**(21), 25866–25879 (2014).
13. Z. Zhang, G. Lu, and F. T. S. Yu, "Simple method for measuring phase modulation in liquid crystal televisions," Opt. Eng. **33**(9), 3018–3022 (1994).
14. D. Engström, M. Persson, J. Bengtsson, and M. Goksör, "Calibration of spatial light modulators suffering from spatially varying phase response," Opt. Express **21**(13), 16086–16103 (2013).
15. A. Serrano-Heredia, P. Purwosumarto, and F. T. S. Yu, "Measurement of the phase modulation in liquid crystal television based on the fractional-Talbot effect," Opt. Eng. **35**(9), 2680–2684 (1996).
16. A. Lizana, I. Moreno, C. Iemmi, A. Márquez, J. Campos, and M. J. Yzuel, "Time-resolved Mueller matrix analysis of a liquid crystal on silicon display," Appl. Opt. **47**(23), 4267–4274 (2008).
17. F. J. Martínez, A. Márquez, S. Gallego, M. Ortuño, J. Francés, A. Beléndez, and I. Pascual, "Averaged Stokes polarimetry applied to evaluate retardance and flicker in PA-LCoS devices," Opt. Express **22**(12), 15064–15074 (2014).
18. X. Xun and R. W. Cohn, "Phase calibration of spatially nonuniform spatial light modulators," Appl. Opt. **43**(35), 6400–6406 (2004).
19. S. Reichelt, "Spatially resolved phase-response calibration of liquid-crystal-based spatial light modulators," Appl. Opt. **52**(12), 2610–2618 (2013).
20. A. Bergeron, J. Gauvin, F. Gagnon, D. Gingras, H. H. Arsenault, and M. Doucet, "Phase calibration and applications of a liquid-crystal spatial light modulator," Appl. Opt. **34**(23), 5133–5139 (1995).
21. C. Kohler, F. Zhang, and W. Osten, "Characterization of a spatial light modulator and its application in phase retrieval," Appl. Opt. **48**(20), 4003–4008 (2009).
22. *http://holoeye.com/spatial-light-modulators/slm-pluto-phase-only/*: Phase Cam Manual.
23. I. Moreno, A. Lizana, A. Márquez, C. Iemmi, E. Fernández, J. Campos, and M. J. Yzuel, "Time fluctuations of the phase modulation in a liquid crystal on silicon display: characterization and effects in diffractive optics," Opt. Express **16**(21), 16711–16722 (2008).

1. Introduction

Parallel-aligned liquid (PAL) crystal spatial light modulators (SLM) are devices for wavefront manipulation that can be considered as linear retarders with spatially-resolved programmable phase-shift. They are core elements in a variety of applications where pure phase modulation is required [1,2], e.g., wave aberration control and ophthalmic simulators [3–7], shaping of femto-second pulses [8], differential interference contrast microscopy (DIC) [9], optical tweezer systems [10] or wavefront sensors [11], among others. Current PAL-SLMs are based on liquid crystal-on-silicon (LCOS) technology. LCOS provide a faster and more precise response than previous electrically- or optically-driven elements, which were considered slow for many phase modulation applications.

Ideally, PAL-SLM phase modulation response should be linear and range at least from 0 to 2π, for the operation wavelength. An additional ideal requirement would be having a uniform phase modulation distribution over the entire SLM surface. In some models, gamma curves can be defined by the user and the average phase response within large areas of the SLM can be adjusted to a 2π range. Other models are provided by the manufacturer with a linearized average phase response. Nevertheless, in those applications requiring high precision for the control of the phase, linearity, and uniformity in the phase depth range, evaluation is required to properly operate the device, or even to correct its predefined phase response. Undesired phase artifacts might also arise under certain conditions [12].

A number of calibration procedures have been described in the literature. Among them, procedures based on diffractive gratings [13,14], fractional Talbot images [15], Mueller matrix parameters [16,17], intensity transmission between crossed polarizers [3,18,19], interferometry [19,20], or back-propagation phase retrieval techniques [21] can be found. The two-beam interference technique is widely employed since it is recommended by some suppliers (e.g. Holoeye Photonics AG, Germany) as a relatively simple and precise method for calibrating SLMs [22]. It involves projecting two circularly shaped beams which are laterally displaced (several mm) onto each half of the SLM. These beams are then overlapped by means of a lens in order to produce a Young interference pattern that is imaged onto a camera by using a microscope objective that increases the size of the fringes. The movement of the pattern when applying a varying voltage (coded as a gray level image) to one side of

#265379 Received 18 May 2016; revised 10 Jun 2016; accepted 10 Jun 2016; published 15 Jun 2016

the SLM can be used to calibrate phase production in the SLM. Dedicated software is provided by some manufacturers for automatically performing the calibration. Despite the apparent simplicity of such method, its practical implementation can be demanding. The use of a lens for overlapping small spots, the need of a microscope objective for magnifying the fringes, and the fact that the interfering beams travel along paths relatively far away compared to the wavelength (typically millimeters compared to hundreds of nanometers) before overlapping implies that fringe patterns become very sensitive to any change on their path difference introduced by mechanical vibrations and even air turbulence. Another major difficulty arises when aligning the system since errors when overlapping the focal spots produced by the two beams can reduce considerably the contrast of the fringes and can affect the measurements. Thus, this apparent simple procedure is time consuming, requires precise alignment involving several optical components for reasonable phase estimation. On the other hand, the method becomes practically insensitive to phase flickering [23] provided that a long enough exposure time is used, and it is considerably independent to non-linearities of the camera response, since phase measurement relies on pattern shift and not on intensity. In other words, the method directly yields average phase modulation without being affected by phase flickering. This could be regarded as advantageous from the point of view of data processing and system simplicity. Nevertheless, phase flickering cannot be estimated straightforwardly from this method (although it is expected to impoverish the contrast of the produced fringes to some extent) and it constitutes a limitation if its effect has to be precisely evaluated.

Intensity transmission methods [3,18] are able to provide spatially resolved [14,18,19] images of phase modulation induced by birefringence changes. The procedure based on intensity transmission itself does not provide all the initial phase terms related to glass thickness, or alternatively flatness, variation. Thus, the latter method can be combined [18] with an interferometric system to properly retrieve such parameter. Phase modulation estimation with that approach is robust against vibration and air flow, since it is not strictly dependent on beam interference. This property is however lost in the initial phase estimation when interferometric approaches are used. Nevertheless, an extra polarizer (analyzer), a linear sensitivity camera and additional optics after the SLM are required as well. Other drawbacks are that only phase terms corresponding to birefringence variation are retrievable (not sensitive to phase contributions coming from glass cover thickness or other terms, as commented), as well as some degree of dependence on phase flickering. From the point of view of computation of phase, it also implies an important drawback. Specifically, intensity images depend on cosine of the effective phase difference of liquid crystal molecules. Phase difference does not evolve linearly in general, and registered intensity is also affected by gamma parameter of the recording camera. It might lead to misevaluated phase values by simply applying the arccosine function or even when fitting it to the cosine of a linear phase, as it will be discussed later. Thus, proper phase estimation with this method should require much more sophisticated computational techniques.

In general, all of the involved methods have advantages and disadvantages, but they require some optical components and relatively good alignment. The method proposed here relies entirely on the SLM itself to create spatial patterns which will directly lead to phase modulation estimations without requiring any optical element. The new proposed method has been experimentally tested with a commercially available SLM unit (PLUTO, Holoeye Photonics AG, Germany).

The paper is organized as follows: In section 2 the new procedure and optical system for calibration are described. In section 3 a phase linearization procedure for the PLUTO SLM with this method will be described. In section 4 a comparison with other calibration methods is provided. In section 5 a spatial phase calibration and correction test is presented. Finally, section 6 summarizes the main conclusions of the work.

#265379 Received 18 May 2016; revised 10 Jun 2016; accepted 10 Jun 2016; published 15 Jun 2016

2. Optical system and calibration procedure

Figure 1 shows a schematic representation of the calibration system. A 532-nm laser diode (CPS532, Thorlabs Inc., USA) was used as light source. Light was focused by a microscope objective (OBJ), filtered by a pinhole aperture (PH) and collimated by a 150-mm focal-length lens (L). Proper polarization selection of light, parallel to liquid crystal director (horizontally polarized light in this case), was carried out by polarizer P. SLM is the spatial light modulator to be calibrated, a model PLUTO-VIS (Holoeye Photonics AG, Germany). Intensity patterns were collected by a CMOS camera, (DMK72AUC02, Imaging Source Europe GmbH, Germany).

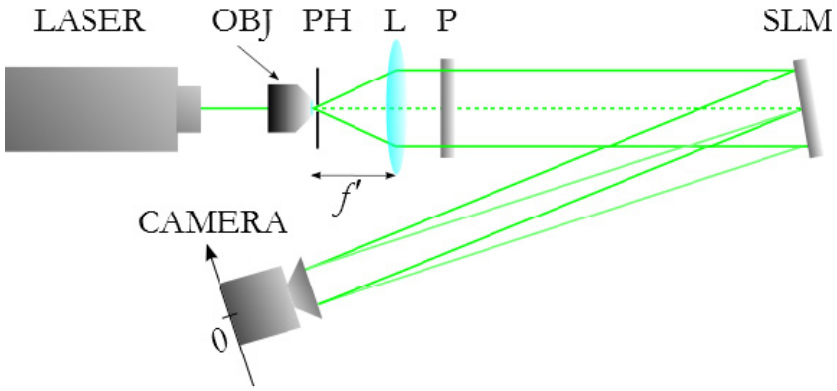

Fig. 1. Diagram of the phase calibration system. OBJ is a microscope objective, PH stands for a pinhole, L is a collimating lens and P is a polarizer. The dotted line represents the optical axis before the SLM. Darker green line after the SLM represents the non-deflected light reflected back from the uniform part of the SLM. Light green line represents one of the tilted 'plane' waves (+ 1 order, for example) reflected back from the part of the SLM encoding the binary grating (the −1 order is not depicted since it is deflected to the left and interferes nowhere). This wave interferes with the other wave at the camera plane creating interference fringes.

The principle of operation of the method relies on the ability to produce spatially varying phase patterns onto the SLM screen and their subsequent effect on plane wave propagation. Specifically, two different phase patterns were simultaneously sent to the SLM: half the screen was addressed with a uniform gray level, which we will call 'piston' phase, whose value was varied during the calibration procedure, while the other half reproduced a binary vertically-oriented diffraction grating that remained static along the calibration process. The name 'piston' is related to the first Zernike polynomial, which represents a constant phase term, which in our scheme depends on the addressed gray level to the uniform part of the SLM. Thus, from now on, we will refer to the presented procedure as 'piston/grating' calibration method. Examples of the mentioned combined patterns are shown at the left column of Fig. 2.

Illuminating the previously described phase structures with a collimated beam produces an interferometric scheme: The binary grid acts as a diffraction grating and, ideally, splits 80% of the energy of the collimated beam into the diffraction orders ± 1 (40% each), with angles, dependent on the grid period, that bring one of them to overlap with the beam reflected on the uniform half of the SLM producing a fringe pattern. The piston gray level modifies the optical path traveled by the corresponding reflected beam and thus displaces the interference fringes proportionally to the added phase. Thus, the light coming from the piston part (non-deflected plane wave) carries the phase shift information of the SLM, while one of the tilted plane waves coming from the grating part is used as a reference interfering beam. The right column of Fig. 2 shows examples of experimental fringes obtained, corresponding with the phase maps at left column. The change in the position of the fringes can be better appreciated with the help of a vertical red line on Fig. 2. The relationship between displayed gray level and added phase can be obtained by determining the fringe position.

#265379 Received 18 May 2016; revised 10 Jun 2016; accepted 10 Jun 2016; published 15 Jun 2016

For the gray level selection of the bars in the diffraction grating, a set of bars in the grating were set to zero gray level while the gray level of the remaining group of bars was experimentally chosen. Since prior knowledge of phase production properties of the SLM may be inexistent or incorrect in a real experimental situation, the calibration procedure was designed to work without a-priori information. The grid gray level of the remaining set of bars of the grating was scanned until the contrast of the observed interference fringes was visually maximized on the camera image. Maximum contrast would occur, in fact, when the phase difference between bars in the grating is π radians, regardless of piston gray level. However, if this value is not exactly reached, the result would be a reduction on the diffracted beam intensity resulting in a loss of contrast but the fringe movement, which is the basis of the calibration procedure, should not be affected. This step needs to be performed before the phase shift estimation procedure.

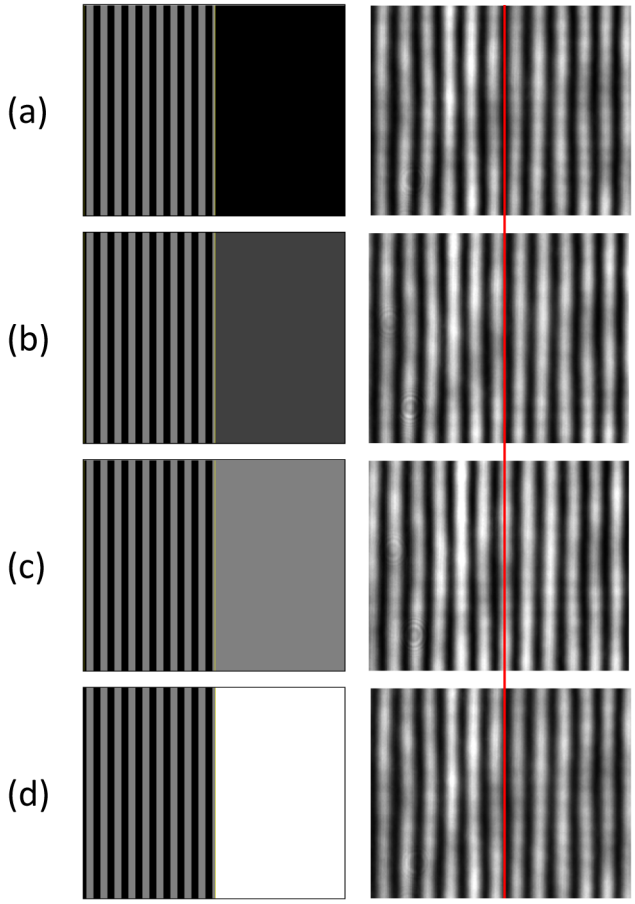

Fig. 2. Examples of addressed phase maps (left) and corresponding experimental fringe patterns (right) for different piston gray levels: (a) 0, (b) 64, (c) 128, and (d) 255. A red line is added to evidence fringe displacement.

The intensity in the fringe pattern varies along the horizontal coordinate, x, as:

$$I(x,g) = I_0 + \Delta I \cdot \cos\left(2\pi \cdot x/P + \phi_0 + \Delta\phi(g)\right), \quad (1)$$

where I_0 and ΔI are the interference intensity terms, P is the spatial period of the interference fringes, ϕ_0 is the initial phase value (irrelevant for several applications), and $\Delta\phi(g)$ is the

#265379 Received 18 May 2016; revised 10 Jun 2016; accepted 10 Jun 2016; published 15 Jun 2016

phase added as a function of gray level g, in the piston section of the SLM, which is in fact the relationship searched for with the calibration procedure.

Fringe period, P, must be appropriately chosen. The bigger this parameter, the less sensitive to disturbances the procedure is expected to be, as it has been experimentally tested. In the two beam interference calibration method [20,22], P is a function of wavelength λ, distance between beams d, and focal length of the focusing lens f'. Just to provide an order of magnitude, for two 550-nm beams 3 mm apart focused by a 10-cm focal-length lens, the fringe period would be given by:

$$P_{two\ beams} \approx \frac{\lambda \cdot f'}{d} = 18 \mu m. \tag{2}$$

In contrast, the period of the fringes in the proposed method depends on the tilt angle introduced in the diffracted beam, which is controlled by the size of the bars in the left part of the phase maps in Fig. 2. Using the diffraction grating equation, i.e. senθ = λ/P, for determining the first order diffracted angle and the relationship between tilt angle and optical path difference, it follows that period P of interference fringes coincides with the grating period (or it is comparable to it if normal incidence is not used). As an example, for a grating composed of 8-pixel-wide bars (grating period, N = 16 pixels) on an SLM with pixel size s = 8 μm, such as the PLUTO SLM, the fringe period would be:

$$P_{grating} = N \cdot s \approx 128 \mu m, \tag{3}$$

which is more than six times higher than the previous period and therefore, the fringe pattern would be less affected by vibrations. Furthermore, this number could be increased simply by addressing larger grating periods. Apart from this feature, since reflected beams start to overlap at zero distance, it is possible to achieve a fringe region at shorter distances minimizing the possible impact of air turbulences.

In either case, the ratio between fringe displacement for a given piston gray level, g, and fringe period equals $\Delta\phi(g)/2\pi$. Therefore, the added phase function can be obtained from a series of images with varying gray level in the uniform part of the SLM.

Fringe displacement can be simply computed by determining the position of the fringe maxima. Therefore, wider the fringes will increase accuracy. As a possible alternative, we propose a Fourier transform-based method: The Fourier transform of a sinusoidal grid contains two impulses (peaks) at the corresponding spatial frequency, whose argument depends on the fringe position due to the shift property. This approach allows for theoretically detecting effective displacements smaller than one pixel. Figure 3(a) shows, as an example, the modulus of the discrete Fourier transform (DFT) for an experimental fringe pattern, with the two-peak structure in evidence at the corresponding spatial frequencies. The mean intensity in the fringe pattern was subtracted prior to the Fourier transform in order to remove the peak at spatial frequency 0. Figure 3(b) shows the phase modulation function, $\Delta\phi(g)$, for a PLUTO SLM. Fringe displacement was obtained from change in the argument of the right-hand side impulse (positive spatial frequency) relative to the initial gray level, g = 0. Due to the cyclic nature of the argument, phase jumps might appear on the retrieved curve. In that case, proper 2π additions or subtractions (phase unwrapping) can be applied in order to enforce curve to be continuous.

#265379 Received 18 May 2016; revised 10 Jun 2016; accepted 10 Jun 2016; published 15 Jun 2016

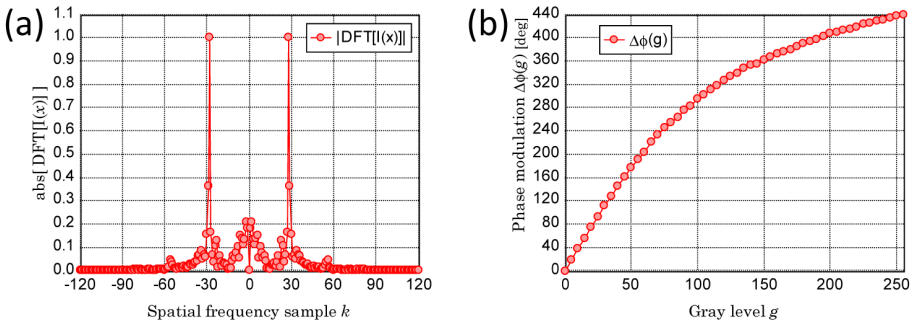

Fig. 3. Panel (a): Modulus of the discrete Fourier transform (in normalized units) for a given fringe pattern after subtracting the mean intensity. Panel (b): Phase modulation (degrees) relative to gray level 0, obtained from the argument of the right side impulse of the Fourier Transform.

3. Linearization process for PLUTO SLMs

This method allows a straightforward procedure to linearize the phase response of a SLM. A PLUTO SLM unit was linearized as an example. For this purpose, simple steps were devised. These steps did not require other information but the actual preloaded gain or gamma curve, $\gamma_p(g)$, which otherwise should preferably be a linear profile. This is the case because in the PLUTO SLM the gamma curve is loaded into the driver's internal memory and the new curve, obtained from the calibration procedure, will overwrite the old one. In other SLM models, the initial gamma curve is a factory setting that cannot be externally accessed and remains a fixture. In that case, no explicit knowledge about it is required for the calibration procedure and the new gamma curve can be applied externally in the control software.

Once the phase profile, $\Delta\phi_p(g)$, for the initial gamma setting, $\gamma_p(g)$, was measured, both data sets were interpolated to a convenient number of data points (e.g. 1024), and a conversion table was created between them. Using this table in reverse, the corrected gamma curve, $\gamma_c(g)$, was constructed by associating to each gray level, g, the gamma value that induced a phase $2\pi / g$ radians. In our experience, the linearization procedure produced better results when the phase production range is slightly but no much above 2π radians. For PLUTO SLM, this range can be modified by means of two voltage settings in the driver's internal memory (V_{bright} and V_{dark}) [22].

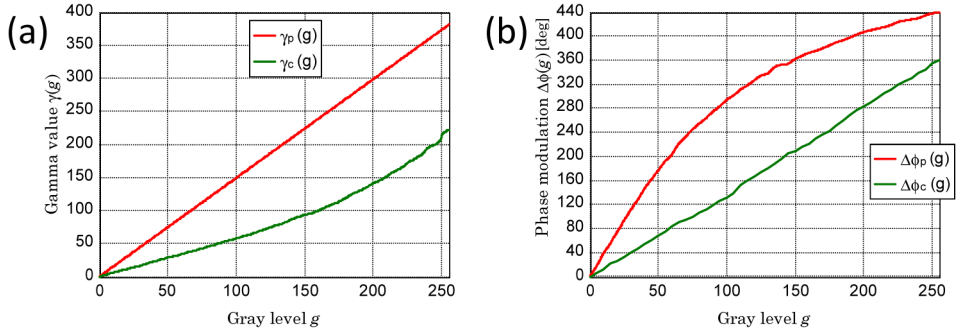

Fig. 4. Panel (a): preset (linear) gamma curve (red) and phase (degrees) linearization gamma curve (green). NOTE: Gamma values are integers inside a range dependent on the SLM driver configuration and should only be used to compare shapes. Panel (b): Experimentally determined phase modulation curves in degrees before (red) and after (green) linearization.

Figure 4 illustrates an example of phase correction with the described procedure. The experimental phase modulation curve obtained for a linear gamma curve (red lines in panels (a) and (b), respectively) was used for associating to each gray level the gamma value that

#265379 Received 18 May 2016; revised 10 Jun 2016; accepted 10 Jun 2016; published 15 Jun 2016

produces the correct phase for a linear behavior, after interpolation in order to avoid possible large experimental-phase steps reducing precision. The corrected gamma curve, $\gamma_c(g)$, was then loaded into the SLM driver and the resulting phase modulation curve was measured and found linear (see green lines).

4. Comparison with other calibration methods

In this section, the new calibration procedure is compared to other existing methods. Figure 5(a) shows three experimentally obtained phase curves by means of the two beam interference method [22] (blue line), the diffraction grating method [13] (red line) and new piston/grating proposal (green line). These results were retrieved with driver settings (including gamma curve) provided by the manufacturer to produce a linear response for a longer wavelength than the one used in this work, hence the phase production range above 360° (2π radians). It can be seen that both the new piston/grating method and the diffraction grating method provided similar results. The linear phase curve retrieved by two beam interference was slightly below the other two. The two-beam method slightly underestimated the phase production range possibly due to slight local inhomogeneities or sensitivity to vibrations/turbulence, since neither stabilization nor air isolation was used.

Figure 5(b) illustrates a comparison between the piston/grating method and the intensity transmission [3,18] measurements performed after the phase linearization process presented in this work was carried out. The latter method is not intended for linearization but for estimating the phase production range, by fitting a sinusoidal function to the transmitted intensity when the SLM is set between crossed polarizers at 45° and ± 45° respect to the director of liquid crystal molecules. The experimental intensity values (symbols) in normalized units can be compared to the cosine of the phase values provided by the piston/grating method (line) conveniently shifted. In other words, a phase offset was added to phase modulation coming from our method to minimize difference between such methods. This constant phase stands for the initial phase due to birefringence at zero gray level the intensity transmission method is sensitive to, but it does not affect at all to relative phase modulation yielded by these methods, which is being compared. Both methods were in good agreement. The main differences visible around the maximum and minimum intensity levels might be caused by camera non-linearities, polarizer imperfection, and phase flickering [23] affecting the transmitted intensity.

Some of the main drawbacks of the two-beam method were commented previously. When dealing with binary grating phase estimation, it has a good mechanical and air flow stability, which is intrinsic to diffraction-based approaches. Some of the inconvenients are that a high dynamic range and linear sensitivity intensity sensor as well as a Fourier transform lens are required. This approach is also affected by temporal phase fluctuations. The same pros and cons would apply to the intensity transmission method.

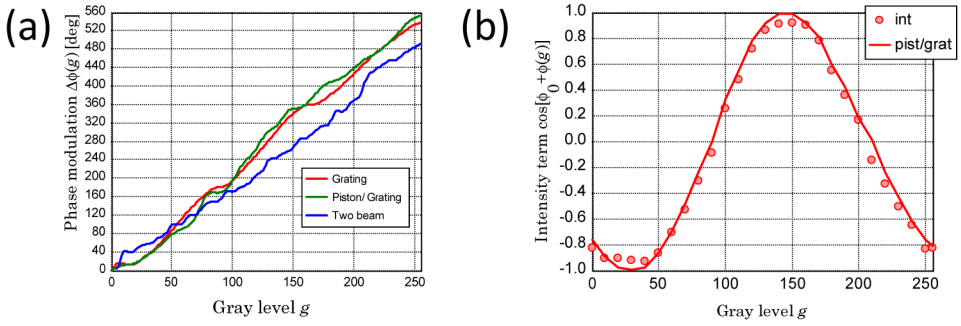

Fig. 5. Comparison of the piston/grating method with previously described methods for SLM calibration. (a) Phase modulation curves estimated (degrees) with a two-beam interferometric scheme (blue), a diffraction grating-based procedure (red) and the new method (green). (b) Transmitted intensity between crossed polarizers (circles) compared to the cosine of the induced phase estimated with the new method (line).

#265379 Received 18 May 2016; revised 10 Jun 2016; accepted 10 Jun 2016; published 15 Jun 2016

5. Spatially-resolved phase modulation calibration

The piston/grating method can be modified to provide a spatially-resolved phase-modulation calibration of the SLM. In order to prove the concept, a simple strategy is shown in this section and results are compared to the spatially-resolved version of the intensity transmission method.

In order to match SLM coordinates and camera coordinates, a series of phase patterns (see Fig. 6(a) for an example) consisting of a rectangular array of circular pupils of 128-pixel diameter, set to a constant gray level, and surrounded by a random phase mask, were addressed to the SLM in phase modulation mode. Either even or odd-ordered pupils were hidden each time (resembling a 'chess table' arrangement). Random background is changed each time as well. The reason for switching off alternate pupils is that 'imaged' pupils (diffraction coming from them indeed) get affected by surrounding neighbor pupils, and more defined pupil images at the camera plane are obtained when alternating them. Assuming that a collimated beam impinges the SLM screen, the effect of this mask for a single pupil in it is the following: random phase background scatters incoming light in all directions while the light impinging the circle keeps its direction so that the SLM behaves like a programmable position pupil. This way, a correspondence between SLM and camera coordinates can be established. Thus, after averaging all the alternate even/odd images captured by the camera, the result presented a ring-like array structure that can be seen in Fig. 6(b). The ring positions (centroids) together with the known positions of the pupils in the phase pattern were used to establish the correspondence between SLM and camera coordinates. Only the central 640 x 384 pixels of the SLM were imaged in the example.

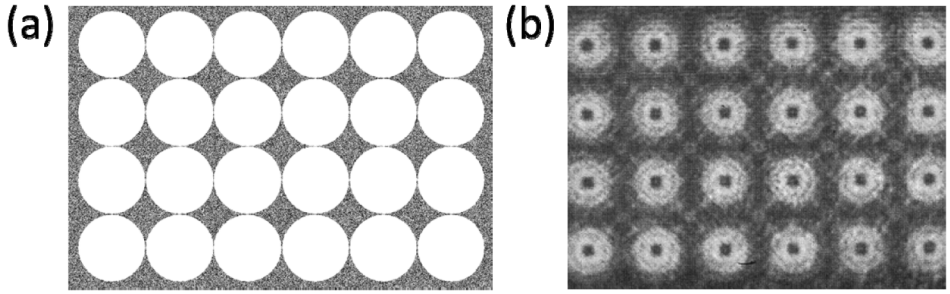

Fig. 6. (a) Example of pupil array pattern surrounded by random phase values sent to the SLM. (b) Mean intensity pattern obtained by averaging the recorded images for a set of phase patterns.

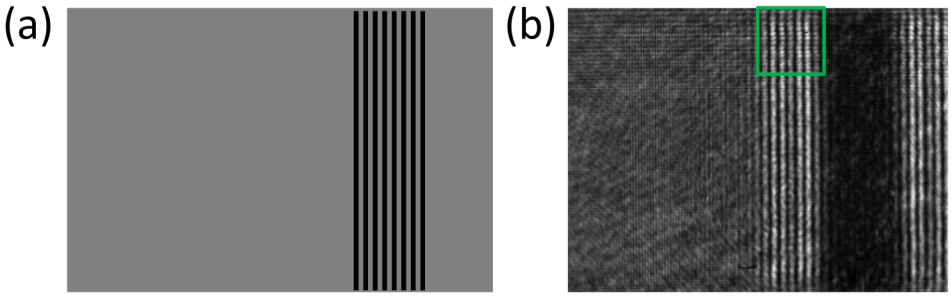

Fig. 7. (a) Example of spatially-resolved calibration pattern. (b) Corresponding experimental fringe image. The green square represents the selected measurement area at the camera plane. This interest region is changed each time to evaluate the phase modulation at different regions of the SLM. This way, a single column grating at the SLM enables for measuring phase at different regions.

#265379 Received 18 May 2016; revised 10 Jun 2016; accepted 10 Jun 2016; published 15 Jun 2016

The spatially-resolved calibration masks consisted of a 128-pixel wide column of vertically aligned binary bars (period 16 pixels) on a piston background of varying gray level. The column position was changed in order to test different sections of the SLM. An example is shown in Fig. 7(a). As a result, this phase mask produces two regions of vertical fringes. Each fringe region corresponds to the overlapping of orders ± 1 with the beam reflected from the uniform gray level area (see Fig. 7, panel b). As the piston gray level was changed, the fringes at each side moved in opposite directions. Taking into account such displacement, phase dependence on gray level at fringe regions can be determined using Fourier analysis. In order to spatially analyze phase modulation, each fringe column was divided in 128x128 pixel blocks, which can be regarded regions of interest where phase modulation is evaluated each time. The size of these blocks can be either reduced or increased as a matter of trade-off between spatial resolution and measurement noise. The minimum size of squares is also expected to be limited by diffraction efficiency issues. The center of each block was selected to coincide with the centroid of each pupil at the camera plane. As an example, one of these square blocks is depicted in Fig. 7(b). It has to be mentioned that a single grating column enables this way to spatially calibrate different regions of SLM.

Figure 8 illustrates an example of spatially-resolved calibration for a section of a PLUTO SLM. The color map represents phase variation with regard to average phase across the area for gray level g = 255, $\overline{\Delta\varphi_{255}(x,y)}$ = 365° (values ranging from 375° to 360°). For visualization purposes, cubic splines were used to interpolate the results obtained in 128x128-pixel cells. The relative standard deviation was 0.83%, which could be regarded as a good phase modulation uniformity indicator.

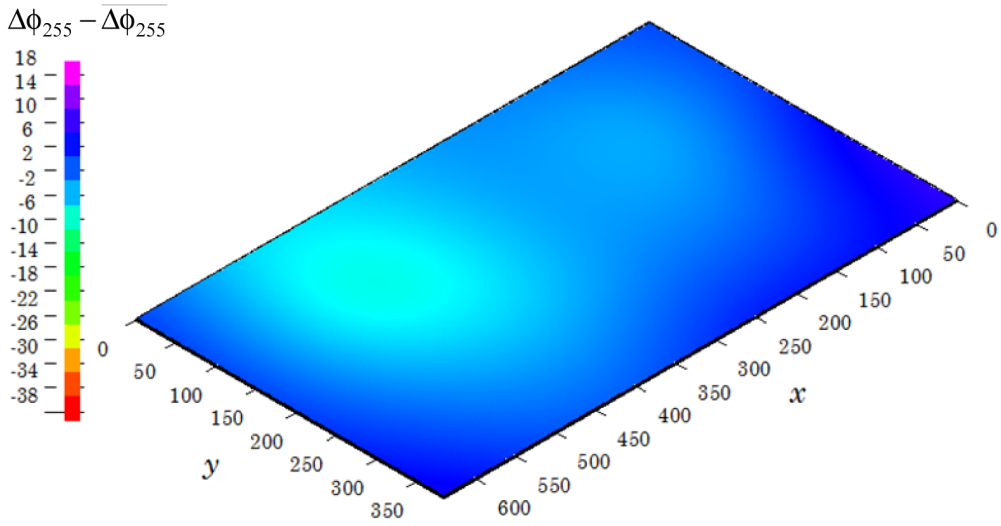

Fig. 8. Spatial differences in phase modulation depth with respect to the spatial average. Values were obtained in 128x128-pixel cells and interpolated with cubic splines to produce a smooth profile.

The intensity transmission method permits estimating the spatial phase modulation of a given SLM without requiring a rather complex modification of the optical set up. Thus, we decided to extend the comparison in previous section to the results provided by piston/grating method at the calibration area of the SLM that fitted into the camera.

To extract phase modulation information from intensity transmission method, the following function was used to fit the experimental data:

$$f(x,y,g) = \cos\left(\Delta\phi_{255}(x,y)\, g/255 + \phi_0(x,y)\right) \tag{4}$$

This model makes three assumptions:

#265379 Received 18 May 2016; revised 10 Jun 2016; accepted 10 Jun 2016; published 15 Jun 2016

1. Phase modulation is approximately constant with time.

2. Phase modulation can be given by a linear term.

3. Detector (camera) response is approximately linear with intensity.

Figure 9 shows the cosine terms of the intensity modulation produced with crossed polarizers at different SLM areas, which are specified by fringe images at the right topmost part of each graph. Representation of cosine terms was chosen instead of computed phase, since comparison of both methods to experimental data is simpler this way. Different information is depicted in each graph. First, circles correspond to the experimental values of the cosine term, retrieved from camera images. The fitted results with the previous described model are depicted as red lines in Fig. 9. An equivalent cosine term is depicted as well when using the phase modulation $\Delta\phi(x,y,g)$ provided by the piston/grating method instead (blue lines). This method makes no assumptions about phase behaviour. In this case only the term $\phi_0(x,y)$ is missing and needs to be fitted.

We observed that the piston/grating data (blue lines) qualitatively agree better than the linear phase model to the experimental data of the cosine of phase. In addition, the root mean square (RMS) error for all stored data has been estimated as 0.070 for the piston/grating approach, and 0.091 for the linear phase fitting (normalized units ranging from −1 to 1 are used), as numerical justification for previous statement.

At first glance, one could think that in spite of the error values provided, direct phase retrieval intensity measurements should yield not so different results from piston/grating data. Nevertheless, when extracting and comparing phase modulation information from both methods, we have observed they do not provide exactly the same results, especially when observing the shape of spatial phase patterns.

When directly using intensity measurements for phase estimation, we consider that two choices would provide more accurate results:

- Either time resolved measurements and linear sensitivity detectors [16] are used,
- Or all the non-linear sensitivity and phase fluctuation [23] sources have been somehow characterized in advance, which constitutes a difficult and time consuming procedure.

On one hand, if phase behavior is assumed to be locally linear, which is the simplest approach to deal with and it is often adopted [4], it may lead to not so correct phase estimations. On the other hand, a fringe-based approach, as it is the case of the proposed method, is almost insensitive to any kind of non-linear detector sensitivity and time fluctuation (provided that enough exposition time were used), directly providing mean phase modulation values.

Moreover, the proposed method is capable of providing local phase non-linearities and could allow for performing local phase linearizations by appropriate control software of the device.

#265379 Received 18 May 2016; revised 10 Jun 2016; accepted 10 Jun 2016; published 15 Jun 2016

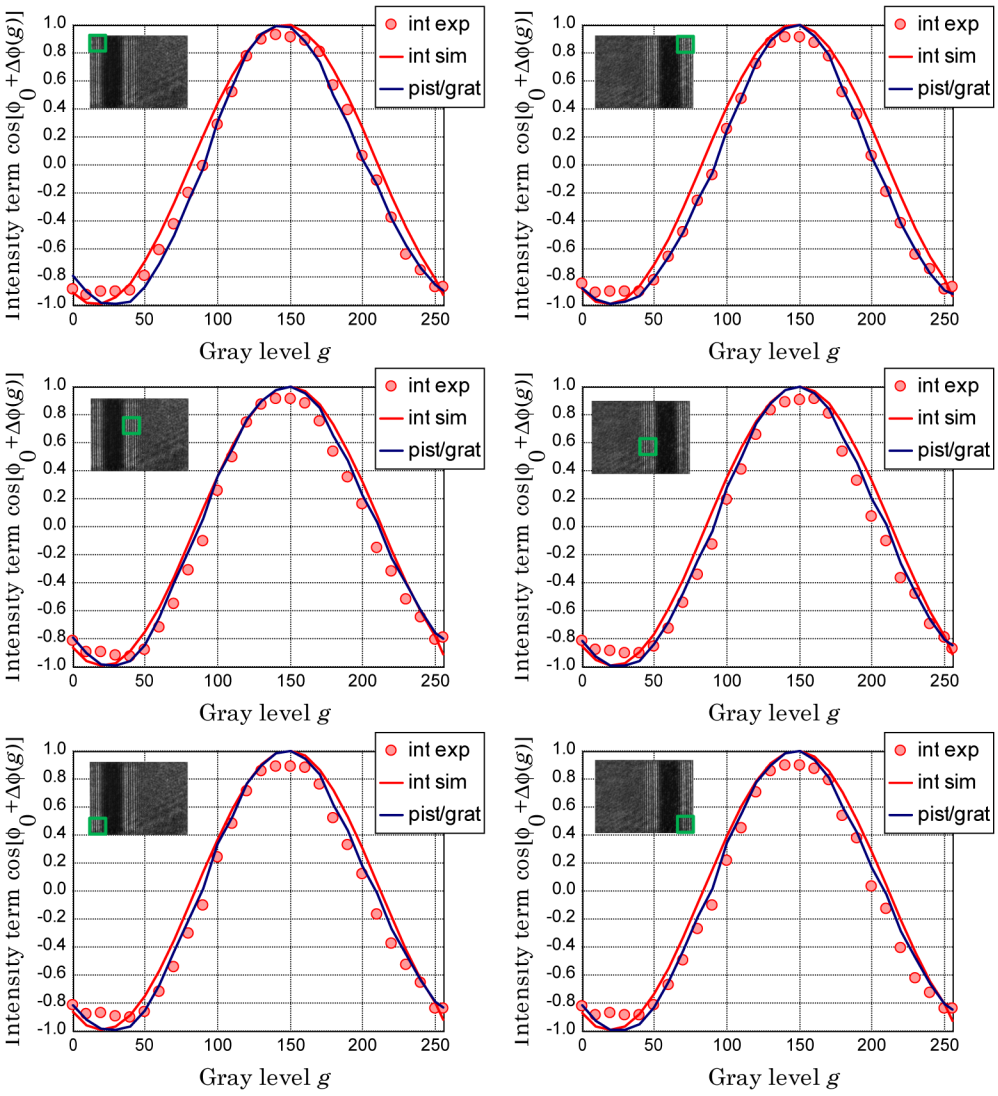

Fig. 9. Fitting between cosines of the phase retrieved from intensity method both experimentally (circles) and fitted (red lines) and the spatially resolved piston/grating method (blue lines) for different fringe-production zones of the SLM. Each zone is depicted at the right topmost part of each graph.

6. Conclusions

In this work, we present a method for phase calibration in LC-SLMs that does not require any optics: Only a collimated beam, a polarizer and a low cost CMOS camera were employed. The method is based on the use of phase profiles directly programmed onto a SLM consisting of the combination of a piston, of varying gray level, and a binary grating. Employed to perform a global SLM calibration over a large area, the new method produces similar results to other existing methods but presents advantages such as relaxing the requirement for precise alignment or very good stability against mechanical vibrations and air turbulence for short working distances. Some convenient properties of the method are:

1. Simplicity to obtain high quality interference fringes.

#265379 Received 18 May 2016; revised 10 Jun 2016; accepted 10 Jun 2016; published 15 Jun 2016

2. No precise alignment required.

3. Estimated average phase values are insensitive to phase flickering when using exposure times long enough. The directly method provides the time-averaged phase modulation function.

4. Higher degree of insensitivity to intensity values in the image (i.e., to camera non-linearities, gamma curves, or even peak saturation) compared to polarimetric methods. The estimated phase is mostly dependent on shape positions, not on intensity.

5. Higher robustness against optical path disturbances when wide enough bars are used for the diffraction grating in the SLM. As a result, mechanical vibration stabilization is not required.

6. Minimal effect of air turbulence since the set up can operate with short propagation distances.

The method shares characteristics with interferometric methods (insensitivity to temporal fluctuations of the SLM and to intensity settings of the detector) and diffractive methods (robustness against vibration and air turbulence).

With a slight modification, the present method has been shown to perform spatially-resolved calibration data. Some other variations of the method, currently being studied, could give room for estimating the optical flatness of calibrated devices. Moreover, since the method is sensitive to local phase non-linearities, it could also enable for spatial linearization of the phase response. This linearization should be software-based since up to our knowledge current modules only enable for overall average linearization.

Acknowledgments

This research has been supported by the European Research Council Advanced Grant ERC-2013-AdG-339228 (SEECAT) and the Spanish SEIDI, grant FIS2013-41237-R, the European Regional Development Fund (EU-FEDER) and Fundación Séneca Agencia de Ciencia y Tecnología de la Región de Murcia (Spain), grants 18964/JLI/13. Jose Luis Martinez Fuentes acknowledges the conferment of a VALID fellowship (APOSTD/2014/100) from the Government of Valencia (Spain).

#265379 Received 18 May 2016; revised 10 Jun 2016; accepted 10 Jun 2016; published 15 Jun 2016